Transition Metal Chemistry (2019) 44:269–273
https://doi.org/10.1007/s11243-018-0291-8

Kinetics and mechanism of the redox reaction of *N*,*N*′-phenylenebis-(salicylideneiminato)iron(III) with oxalic acid in mixed aqueous medium

I. Ibrahim[1] · **S. O. Idris**[1] · **I. Abdulkadir**[1] · **A. D. Onu**[2]

Received: 3 September 2018 / Accepted: 15 November 2018 / Published online: 3 December 2018

Abstract

The kinetics of electron transfer between *N*,*N*′-phenylenebis-(salicylideneiminato)iron(III), hereafter referred to as $[Fe(Salphen)]^+$, and oxalic acid was studied in mixed aqueous medium (DMSO:H_2O; 1:4 v/v) under pseudo-first-order conditions at 26 ± 1 °C, $I = 0.2$ coulomb^2 mol dm^{-3} (NaCl) and $\lambda_{max} = 435$ nm. The reaction was found to be second order overall and acid independent, and displayed zero Brønsted–Debye salt effect. There was no evidence for the formation of an intermediate complex or free radicals during the reaction. Overall, the kinetic data suggest an inner-sphere mechanism for the reaction, which is first order in both reactants. A plausible reaction mechanism is proposed.

Introduction

Metallo-salen complexes have been extensively used as catalysts for a broad range of transition-metal-catalyzed reactions including epoxidation of olefins, hydroxylation, lactide polymerization and asymmetric ring opening of epoxides [1]. The oxidative nature of metallo-salens has also been exploited for the development of novel chemical nucleases [2–6]. Various metallo-salen complexes are also capable of hydrolytic cleavage of DNA and RNA [7]. As DNA-interacting molecules find potential applications in anti-tumor therapy, intense research efforts are currently being invested toward the development of novel DNA/RNA modifiers and understanding their molecular mechanisms of action [8–10].

Oxalic acid is the simplest dicarboxylic acid, with the formula HO_2CCO_2H. It is a much stronger acid than acetic acid and is also a strong reducing agent [11]. Its conjugate base, the oxalate dianion ($C_2O_4^{2-}$), is a chelating agent for many metals, for example platinum(II) in the drug oxaliplatin [12]. Oxalic acid and oxalates can be oxidized by permanganate in an autocatalytic reaction [13]. Redox reactions involving oxalic acid have been studied [11, 14, 15].

In spite of these and numerous other uses, the redox reaction of the complex, $[Fe(Salphen)]^+$ (salphen = bis(salicylidene)phenylenediamine), with oxalic acid has not yet been reported. The present study has therefore been carried out to obtain kinetic data with a view to gaining insight into the mechanism of this redox reaction.

Materials and methods

All the reagents used were of Analar grade. Reaction rates were monitored by following the decrease in absorbance of the reaction mixture at 435 nm on a CORNING colorimeter 253. Conductivity measurements were taken with a HANNA HI 4321 conductivity meter. Oxalic acid (JHD) was used as the reducing agent, while sodium chloride (M&B) was used to maintain the ionic strength of the reaction medium.

Bis(salicylidene)phenylenediamine and the *N*,*N*′-phenylenebis(salicylideneiminato)iron(III) complex [Fe(Salphen)]Cl were synthesized and characterized according to the published procedures [16]. The structure of the complex is shown in Scheme 1. The Schiff base was prepared by refluxing *o*-phenylenediamine (BDH, 1.71 g, 15.8 mmol) with salicylaldehyde (Merck, 3.3 ml, 31.6 mmol) in methanol (Merck, 30 ml) for 1 h. The precipitate was collected by filtration after cooling, washed with methanol and dried in a desiccator: yield 4.29 g (86%).

The complex was prepared by stirring a mixture of the Schiff base (0.78 g, 2.5 mmol) with anhydrous ferric chloride (SureChem, 0.4 g, 2.5 mmol) in methanol (20 ml)

✉ I. Ibrahim
ibrahimmismaila@gmail.com

[1] Department of Chemistry, Ahmadu Bello University, Zaria, Nigeria

[2] Department of Chemistry, Federal College of Education, Zaria, Nigeria

Scheme 1 Structure of *N*,*N*′-phenylenebis(salicylideneiminato)iron(III)

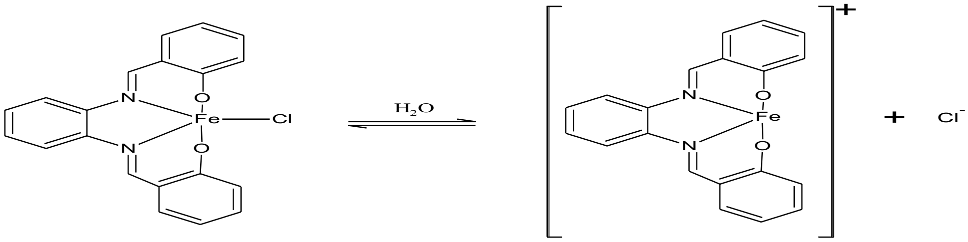

at 60 °C for 30 min, then keeping the mixture at room temperature overnight to precipitate out the complex. The product was recrystallized from methanol and dried in a desiccator: yield 0.47 g (47%).

The molar conductivity of the complex was determined in 2.0×10^{-4} mol dm^{-3} ($DMSO:H_2O$; 1:4 v/v) solution as 145 S cm^2 mol^{-1} with specific conductance of 29.0×10^{-6} S cm^{-1}, consistent with a 1:1 electrolyte. The existence of $[Fe(salen)]^+$ species in $DMSO–H_2O$ (4:1 v/v) and $CH_3CN–H_2O$ (1:1 v/v) solvent systems has been reported previously [17, 18]. Furthermore, Kurahashi and co-workers reported that the ESI mass spectrum of H_2O coordinated iron(III)salen perchlorate in solution gave a single signal corresponding to $[Fe(salen)]^+$ with loss of both H_2O and ClO_4^- [19].

The stoichiometry of the reaction was determined by spectrometric titration using the mole ratio method. The stoichiometry was evaluated from a plot of absorbance against mole ratio [20]. The kinetic studies were carried out under pseudo-first-order conditions with $[H_2C_2O_4]$ in excess over $[Fe(Salphen)^+]$ at 435 nm, $I = 0.2$ $coulomb^2$ mol dm^{-3}, $T = 26 \pm 1$ °C. Pseudo-first-order rate plots of log $(A_t - A_\infty)$ versus time were drawn (where A_∞ and A_t are the absorbance at the end of the reaction and at time *t*), and from the slopes of the plots, the pseudo-first-order rate constants (k_1) were determined. The second-order rate constants (k_2) were obtained from Eq. 1.

$$k_2 = k_1/\left[H_2C_2O_4\right] \qquad (1)$$

The effect of $[H^+]$ on the reaction rate was investigated by varying the $[H^+]$ between 1.0×10^{-5} and 1.0×10^{-4} mol dm^{-3} (using HCl), while $[Fe(Salphen)^+]$ and $[H_2C_2O_4]$ were kept constant at 2.0×10^{-4} mol dm^{-3} and 6.0×10^{-3} mol dm^{-3}, respectively, at 26 ± 1 °C and $I = 0.2$ $coulomb^2$ mol dm^{-3} [21]. The effect of varying the ionic strength of the reaction medium on the rate of the reaction was investigated in the range of 0.18–0.40 $coulomb^2$ mol dm^{-3}, while the concentrations of the reactants were kept constant at 26 ± 1 °C. The effects of added cation and anion were investigated for $[X] = 1.0–6.0 \times 10^{-3}$ mol dm^{-3} ($[X] = Mg^{2+}$ or AcO^-) at constant $[Fe(Salphen)^+]$, $[H_2C_2O_4]$ and ionic strength. The influence of temperature on the reaction rates was studied in the range of 298–313 K, and thermodynamic parameters were determined at constant $[Fe(Salphen)^+]$, $[H_2C_2O_4]$ and ionic strength.

Spectra of the reaction mixture were recorded after commencement of the reaction and were compared with the spectra of the complex alone over a wavelength range of 400–700 nm. A Michaelis–Menten-type plot of $1/k_1$ versus $1/[H_2C_2O_4]$ was also made. A test for free radicals was made by the addition of acrylamide followed by excess methanol to partially reacted mixtures of $[Fe(Salphen)]^+$ and $H_2C_2O_4$ [22].

Results and discussion

From the stoichiometric studies, the mole ratio of the reaction was found to be 2:3 (Fig. 1) and can therefore be represented by the equation:

$$\begin{aligned} &2\left[Fe(Salphen)\right]^+ + 3H_2C_2O_4 + O_2 \\ &\quad \rightarrow 2\left[Fe(Salphen)\right] + 6CO_2 + 2H_2O + 2H^+ \end{aligned} \qquad (2)$$

A stoichiometry of 1:4 has been reported in the reaction between chromic and oxalic acids [11].

In the kinetic analysis, a plot of $\log(A_t - A_\infty)$ against time t gave a straight line graph, suggesting that the reaction is first order with respect to $[Fe(Salphen)^+]$ (Fig. 2). The order of the reaction with respect to $[H_2C_2O_4]$ was determined by plotting log k_1 against log $[H_2C_2O_4]$. The slope of the resulting straight line was 1.04 (Fig. 3). The value of the

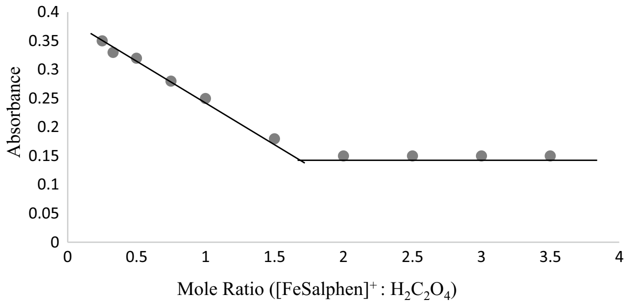

Fig. 1 Plot of Absorbance versus mole ratio for the redox reaction of $[Fe(Salphen)]^+$ and $H_2C_2O_4$ at $[Fe(Salphen)^+] = 2.0 \times 10^{-4}$ mol dm^{-3}, $\mu = 0.2$ $coulomb^2$ mol dm^{-3}, $T = 26 \pm 1$ °C and $\lambda_{max} = 435$ nm

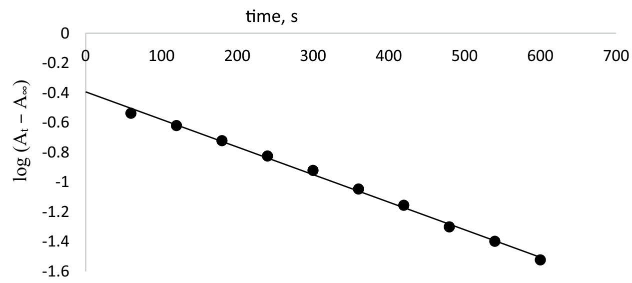

Fig. 2 Typical pseudo-first-order plot for the redox reaction of $[Fe(Salphen)]^+$ and $H_2C_2O_4$ at $[Fe(Salphen)^+] = 2.0 \times 10^{-4}$ mol dm^{-3}, $H_2C_2O_4 = 6.0 \times 10^{-3}$ mol dm^{-3}, $\mu = 0.2$ coulomb^2 mol dm^{-3}, $T = 26 \pm 1$ °C and $\lambda_{max} = 435$ nm

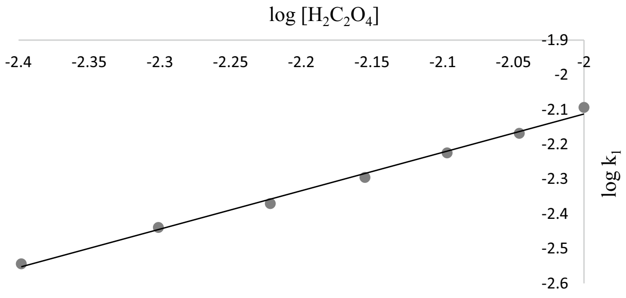

Fig. 3 Plot of log k_1 versus log $[H_2C_2O_4]$ for the redox reaction of $[Fe(Salphen)]^+$ and $H_2C_2O_4$ at $[Fe(Salphen)^+] = 2.0 \times 10^{-4}$ mol dm^{-3}, $\mu = 0.2$ coulomb^2 mol dm^{-3}, $T = 26 \pm 1$ °C and $\lambda_{max} = 435$ nm

Table 1 Pseudo-first-order and second-order rate constants for the reaction of $[Fe(Salphen)]^+$ with $H_2C_2O_4$ at $[Fe(Salphen)^+] = 2.0 \times 10^{-4}$ mol dm^{-3}, $T = 26 \pm 1$ °C and $\lambda_{max} = 435$ nm

10^3 $[H_2C_2O_4]$ (mol dm^{-3})	10 μ, coulomb^2 (mol dm^{-3})	10^3 k_1 (s^{-1})	10 k_2 (dm^3 mol^{-1} s^{-1})
4.0	2.0	2.86	7.15
5.0	2.0	3.64	7.28
6.0	2.0	4.26	7.10
7.0	2.0	5.07	7.24
8.0	2.0	5.96	7.45
9.0	2.0	6.79	7.54
11.0	2.0	8.06	7.33
6.0	1.8	4.28	7.13
6.0	2.0	4.26	7.10
6.0	2.4	4.29	7.15
6.0	2.8	4.27	7.12
6.0	3.2	4.30	7.17
6.0	3.6	4.29	7.15
6.0	4.0	4.26	7.10

Table 2 Effect of acid concentration on the rate of reaction of $[Fe(Salphen)]^+$ with $H_2C_2O_4$ at $[Fe(Salphen)^+] = 2.0 \times 10^{-4}$ mol dm^{-3}, $H_2C_2O_4 = 6.0 \times 10^{-3}$ mol dm^{-3}, $\mu = 0.2$ coulomb^2 mol dm^{-3}, $T = 26 \pm 1$ °C and $\lambda_{max} = 435$ nm

10^5 $[H^+]$ (mol dm^{-3})	10^3 k_1 (s^{-1})	10 k_2 (dm^3 mol^{-1} s^{-1})
0.0	4.27	7.12
1.0	4.29	7.15
2.0	4.28	7.13
4.0	4.26	7.10
6.0	4.29	7.15
8.0	4.27	7.12
10.0	4.28	7.13

second-order rate constant k_2 was fairly constant for different $[H_2C_2O_4]$ and ionic strengths (Table 1). The rate equation for the reaction can be represented by Eq. 3.

$$-\mathrm{d}\left[Fe(Salphen)^+\right]/\mathrm{d}t = k_2\left[Fe(Salphen)^+\right]\left[H_2C_2O_4\right] \quad (3)$$

where $k_2 = 7.29 \pm 0.157 \times 10^{-1}$ dm^3 mol^{-1} s$^{-1.}$

The rate of reaction was found to be independent of $[H^+]$, as shown in Table 2. This observation suggests that the undissociated oxalic acid HO_2CCO_2H is involved in the reaction [11, 14]. The results in Table 1 show that variations in the ionic strength of the reaction medium had no effect on the rate. A plot of log k_2 against $\sqrt{I}$ gave a slope of zero, suggesting a negligible Brønsted–Debye salt effect [23]. This implies that the reaction proceeds via an interaction between uncharged forms of the reactants [24].

The reaction rate was also unaffected by the presence of added ions (Mg^{2+} and AcO^-, Table 3). This result suggests that the reaction follows an inner-sphere mechanism.

We next considered whether an intermediate complex is involved in the reaction. There was no shift in λ_{max} (435 nm) when the spectrum of the reaction mixture was compared with that of $[Fe(Salphen)^+]$. The lack of spectrophotometric evidence for the formation of intermediate complex may suggest an outer sphere mechanism. However, a Michaelis–Menten-type plot of $1/k_1$ versus $1/[H_2C_2O_4]$ was linear with a positive intercept, suggesting the participation of an intermediate complex (Fig. 4) and a possible inner-sphere mechanism.

Addition of acrylamide to the partially reacted solution to serve as a radical scavenger in the presence of large excess of methanol did not produce a gelatinous precipitate. This indicates that the involvement of free radicals in the reaction is unlikely.

The results of temperature dependence experiments are presented in Table 4. A large negative value of $\Delta S^{\ddagger}$ indicates that the species in the activated complex are more ordered, which is evidence for an associative mechanism and an inner-sphere mechanism of electron transfer.

We have analyzed the reaction products as follows. On completion of the reaction, the presence of Fe^{2+} as the

Table 3 Effect of added ions on the rate of reaction of $[\mathrm{Fe(Salphen)}]^+$ with $H_2C_2O_4$ at $[\mathrm{Fe(Salphen)}^+] = 2.0 \times 10^{-4}$ mol dm^{-3}, $H_2C_2O_4 = 6.0 \times 10^{-3}$ mol dm^{-3}, $\mu = 0.2$ coulomb^2 mol dm^{-3}, $T = 26 \pm 1$ °C and $\lambda_{max} = 435$ nm

[X]	10^3 [X] (mol dm^{-3})	$10^3\ k_1$ (s^{-1})	$10\ k_2$ (dm^3 mol^{-1} s^{-1})
Mg^{2+}	0.0	4.26	7.10
	1.0	4.30	7.17
	2.0	4.29	7.15
	3.0	4.29	7.15
	4.0	4.26	7.10
	5.0	4.27	7.12
	6.0	4.28	7.14
CH_3COO^-	0.0	4.28	7.13
	1.0	4.26	7.10
	2.0	4.29	7.15
	3.0	4.27	7.12
	4.0	4.30	7.17
	6.0	4.29	7.15
	8.0	4.26	7.10

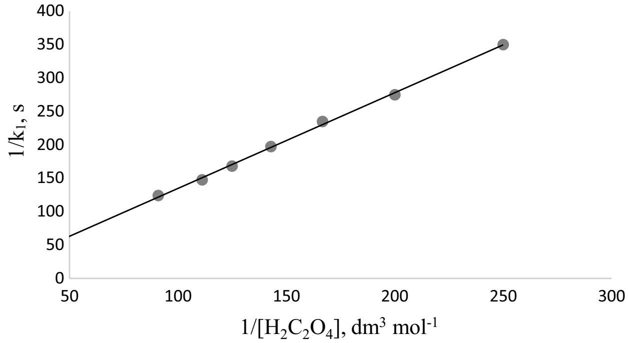

Fig. 4 Michaelis-Menten plot for the redox reaction of $[\mathrm{Fe(Salphen)}]^+$ and $H_2C_2O_4$ at $[\mathrm{Fe(Salphen)}^+] = 2.0 \times 10^{-4}$ mol dm^{-3}, $\mu = 0.2$ coulomb^2 mol dm^{-3}, $T = 26 \pm 1$ °C and $\lambda_{max} = 435$ nm

reduction product of Fe^{3+} was confirmed by mixing the reaction solution with $KMnO_4$ solution. The formation of a brown precipitate indicated the presence of Fe^{2+} [25]. The presence of CO_2, the oxidation product of $H_2C_2O_4$, was confirmed using lime water ($Ca(OH)_2$) which turned milky [26].

On the basis of the results obtained from this investigation, the following reaction scheme is proposed for this reaction:

$$[\mathrm{Fe(Salphen)}]^+ + \mathrm{H_2C_2O_4} \xrightarrow{k_3} [\mathrm{Fe(Salphen)^+//H_2C_2O_4}] \tag{4}$$

$$[\mathrm{Fe(Salphen)^+//H_2C_2O_4}] \xrightarrow{k_4} [\mathrm{Fe(Salphen)}] + 2\mathrm{CO_2} + 2\mathrm{H^+} + \mathrm{e^-} \tag{5}$$

$$[\mathrm{Fe(Salphen)}]^+ + 2\mathrm{H_2C_2O_4} + \mathrm{O_2} + \mathrm{e^-} \xrightarrow{k_5} [\mathrm{Fe(Salphen)}] + 4\mathrm{CO_2} + 2\mathrm{H_2O} \tag{6}$$

For this mechanism,

$$\text{Rate} = k_4[\mathrm{Fe(Salphen)^+//H_2C_2O_4}] \tag{7}$$

Applying the steady-state approximation for the intermediate complex $[\mathrm{Fe(Salphen)^+//H_2C_2O_4}]$,

$$k_3[\mathrm{Fe(Salphen)^+}][\mathrm{H_2C_2O_4}] - k_{-3}[\mathrm{Fe(Salphen)^+//H_2C_2O_4}] - k_4[\mathrm{Fe(Salphen)^+//H_2C_2O_4}] = 0 \tag{8}$$

Then

$$[\mathrm{Fe(Salphen)^+//H_2C_2O_4}] = k_3[\mathrm{Fe(Salphen)^+}][\mathrm{H_2C_2O_4}]/(k_{-3} + k_4) \tag{9}$$

Substituting Eq. (9) into Eq. (7),

$$\text{Rate} = k_3k_4[\mathrm{Fe(Salphen)^+}][\mathrm{H_2C_2O_4}]/(k_{-3} + k_4) \tag{10}$$

Equation (10) is analogous to Eq. (3), where $k_2 = k_3k_4/(k_{-3} + k_4) = 7.29 \pm 0.157 \times 10^{-1}$ dm^3 mol^{-1} s^{-1}.

Conclusion

The redox reaction between *N*,*N′*-phenylenebis-(salicylideneiminato)iron(III) and oxalic acid in mixed aqueous medium (DMSO:H_2O; 1:4) showed a stoichiometry of 2:3. The reaction is second order overall. The rate of the reaction is acid independent and displayed zero

Table 4 Temperature dependence of the rate constants and activation parameters for the reaction of $[\mathrm{Fe(Salphen)}]^+$ with $H_2C_2O_4$ at $[\mathrm{Fe(Salphen)}^+] = 2.0 \times 10^{-4}$ mol dm^{-3}, $H_2C_2O_4 = 6.0 \times 10^{-3}$ mol dm^{-3}, $\mu = 0.2$ coulomb^2 mol dm^{-3} and $\lambda_{max} = 435$ nm

T (K)	$10^3\ k_1$ (s^{-1})	$10\ k_2$ (dm^3 mol^{-1} s^{-1})
299	4.29	7.15
303	4.46	7.57
307	4.94	8.23
311	5.45	9.08
315	8.23	10.15
$\Delta H^‡ = +14.693$ kJ mol^{-1}	$\Delta S^‡ = -198.756$ J mol^{-1} K^{-1}	$\Delta G^‡ = +74.121$ kJ mol^{-1} at 299 K
$E_a = +17.224$ kJ mol^{-1}		

Brønsted–Debye salt effect. Kinetic investigations showed evidence for the formation of an intermediate complex. Based on these observations, an inner-sphere mechanism is proposed as the most plausible mechanistic pathway for this reaction.

References

1. Jacobsen EN, Zhang W, Guler ML (1991) Electronic tuning of asymmetric catalysts. J Am Chem Soc 113:6703–6704
2. Bhattacharya S, Mandal SS (1996) DNA cleavage by intercalatable cobalt bispicolylamine complexes activated by visible light. Chem Commun 13:1515–1516
3. Routier S, Bernier JL, Waring MJ, Colson P, Houssier C, Bailly C (1996) Synthesis of a functionalized salen copper complex and its interaction with DNA. J Org Chem 61:2326–2331
4. Muller JG, Kayser LA, Paikoff SJ, Duarte V, Tang N, Perez RJ et al (1999) Formation of DNA adducts using nickel(II) complexes of redox-active ligands: a comparison of salen and peptide complexes. Coord Chem Rev 186:761–774
5. Czlapinski JL, Sheppard TL (2001) Nucleic acid template-directed assembly of metallosalen DNA conjugates. J Am Chem Soc 123:8618–8619
6. Doctrow SR, Huffman K, Marcus CB, Tocco G, Malfroy E, Adinolfi CA et al (2002) Salen-manganese complexes as catalytic scavengers of hydrogen peroxide and cytoprotective agents: structure-activity relationship studies. J Med Chem 45:4549–4558
7. Komiyama M, Takeda N, Shigekawa H (1999) Hydrolysis of DNA and RNA by lanthanide ions: mechanistic studies leading to new applications. Chem Commun 16:1443–1451
8. Cohen SM, Lippard SJ (2001) Cisplatin: from DNA damage to cancer chemotherapy. Prog Nucleic Acid Res Mol Biol 67:93–130
9. Barnes KR, Lippard SJ (2004) Cisplatin and related anticancer drugs: recent advances and insights. Met Ions Biol Syst 42:143
10. Ott I, Gust R (2007) Non platinum metal complexes as anticancer drugs. Archiv der Pharmazie (Weinheim) 340(3):117–126
11. Zaheer K, Athar AH, Lateef A, Haq MM (1998) Kinetics and mechanism of chromic acid oxidation of oxalic acid in absence and presence of different acid media. A kinetic study. Int J Chem Kinet 30:335–340
12. Ehrsson H, Wallin I, Yachnin J (2002) Pharmacokinetics of oxaliplatin in humans. Med Oncol 19(4):261–265
13. Kovacs KA, Grof P, Burai L, Riedel M (2004) Revising the mechanism of the permanganate/oxalate reaction. J Phys Chem A 108(50):11026–11031
14. Bakore GV, Jian CL (1969) Chromic acid oxidation of oxalic acid: kinetic investigation of the uncatalyzed oxidation of oxalic acid by chromic acid. J Inorg Nucl Chem 31:805–810
15. Subba-Rao PV, Krishna-Rao GSR, Ramakrishna K, Murthy PSN (1991) Kinetics of chromic acid–oxalic acid reaction catalyzed by manganese(II)—kinetic analysis of the consecutive pathway. Indian J Chem 30:239–342
16. Ansari IK, Sahba K, James DG, Mandal SS (2011) Fe(III) salen and salphen complexes induce caspase activation and apoptosis in human cells. J Biomol Screen 16:26–35
17. Liou YW, Wang CM (2000) Peroxidase mimicking: Fe(Salen)Cl modified electrodes, fundamental properties and applications for biosensing. J Electroanal Chem 481(1):102–109
18. Subramaniam P, Vanitha T, Kodispathi T, Sundari CRS (2014) Role of iron(III)-salen chloride as oxidizing agent with thiodiglycolic acid: the effect of axial ligands. J Mex Chem Soc 58(2):211–217
19. Kurahashi T, Kobayashi Y, Nagatomo S, Tosha T, Kitagawa T, Fujii H (2005) Oxidizing intermediates from the sterically hindered iron salen complexes related to the oxygen activation by nonheme iron enzymes. Inorg Chem 44:8156–8166
20. Hamza SA, Iyun JF, Idris SO (2012) Kinetics and mechanism of the redox reaction of toluidine blue and nitrite ions in aqueous acidic medium. Arch Appl Sci Res 4(1):10–18
21. Idris SO, Tanimu A, Iyun JF, Mohammed Y (2015) Kinetics and mechanism of malachite green oxidation by hypochlorite ion in aqueous acidic medium. Am Chem Sci J 5(2):185–193
22. Adetoro A, Iyun JF, Idris SO (2011) Kinetic approach to the mechanism of redox reaction of pyrocatechol violet and nitrite ion in aqueous hydrochloric acid. Res J Appl Sci Eng Technol 3(10):1159–1163
23. Benson D (1969) Mechanism of inorganic reactions in solution, 2nd edn. Mc Graw-Hill, New York City, p 153
24. Atkins PW, de Paula J (2002) Physical chemistry, 7th edn. Oxford University Press, Oxford, p 962
25. Steven Mifsud (2018) MarZ Kreations Malta. http://www.marz-kreations.com/Chemistry/Cation-ID/162k-Iron.html. Accessed 31 Aug 2018
26. Vogel AI (1979) Vogel's textbook of macro and semimicro qualitative inorganic analysis, 5th edn. Longman, London, p 298 **(Svehla G revised edn.)**